JOURNAL OF APPLIED ELECTROCHEMISTRY 19 (1989) 889–896

An investigation of a potential step at a channel electrode

F. LAPICQUE, J. M. HORNUT*, G. VALENTIN, A. STORCK

Laboratoire des Sciences du Génie Chimique–CNRS–ENSIC–INPL, B.P. 451, F-54001 Nancy, France

Received 22 November 1988; revised 23 January 1989

The present paper deals with a theoretical investigation of a potential step at a channel electrode. The study consists in the numerical solution of the partial differential equations relevant to the transient mass balance in the vicinity of the electrode, taking into account the convective term. Although such an equation has been investigated previously for both heat and mass transfer, we present the results obtained with the help of two packages relying upon either the numerical method of lines (DSS/2) or a derived Gear technique (LSODA). Results of the simulation – concentration profile and wall concentration gradient – are reported and a comparison with previous results is carried out. Both packages used yield very similar current variations which are observed to be in a good agreement with experimental data.

Nomenclature

a_0	first coefficient of the power series expansion for the Airy function
b	channel depth (m)
C	concentration (mol m^{-3} or M)
$\mathbf{C} = C/C_b$	reduced concentration
c_0	first term of the power series expansion for the logarithmic derivative of the Airy function
D	diffusion coefficient (m^2 s^{-1})
d_h	hydraulic diameter (m)
F	Faraday constant
$f/2$	friction factor
i	current density (A m^{-2})
I	current (A)
I_L	limiting current (A)
k_d	mass transfer coefficient (m s^{-1})
L	electrode length (m)
Pr	Prandtl number
Re	Reynolds number in the empty channel
s	wall velocity gradient (s^{-1})
Sc	Schmidt number
Sh	Sherwood number
St_m	Stanton number
t	time (s)
T	temperature (K)
T_b	bulk temperature (K)
T_w	wall temperature (K)
$\mathbf{T} = (T - T_b)/(T_w - T_b)$	reduced temperature
t_2	time required for the current to decrease down to twice the steady-state current, following a step of potential (s)
u	local fluid velocity (m s^{-1})
u_m	mean superficial velocity (m s^{-1})
w	channel width (m)
x	axial coordinate (m)
x^+	axial reduced coordinate after [3]
X	axial reduced coordinate (relation 2)
y	coordinate in the normal direction to the electrode (m)
Y	reduced y coordinate (relation 2)
Γ	Gamma function
Γ_w	reduced concentration gradient at the wall $= (\partial \mathbf{C}/\partial Y)_{Y=0}$
$\overline{\Gamma}_w$	reduced concentration gradient at the wall, averaged over the electrode surface
θ	reduced time (relation 2)
θ_2	reduced time corresponding to t_2
τ^+	reduced time after [3]
ν	kinematic viscosity (m^2 s^{-1})

Subscripts

A, B, j	compound
b	bulk
e	electrode
0	standard
∞	steady state

1. Introduction

The transient response induced by a potential step can yield important data for the study of electrode reaction mechanisms or for the measurement of diffusion coefficients. Moreover, such responses in electrochemical reactors are relevant to the behaviour of systems under electrical pulsations. Because of numerous applications in electrochemistry and electrochemical engineering, the transient responses of channel electrodes have been studied by several authors; most of these studies dealt with numerical solution of the differential mass balance relevant to the concentration profile formation in the vicinity of the electrode.

Besides the well-known relation of Cottrell, more recent investigations [1, 2], based on the assumption of a laminar regime in a channel electrode reactor,

0021-891X/89 $03.00 + .12

have taken into account the convective term in the expression for the mass balance which was solved by means of double Laplace transformation. In addition, on the basis of a reversible reaction, A + $ve \rightarrow$ B, these authors have assumed the presence of only A before electrolysis. In addition, a similar equation has been solved by Soliman and Chambré [3] in the field of heat transfer. Yet, double Laplace transformation for heat and mass transfer [1, 3] leads to a simple expression of the flux at the wall in the form of an Airy function and the profiles of concentration – or temperature – cannot be easily obtained. Furthermore, Soliman and Chambré proposed the time variation of the dimensionless local heat flux from which the overall flux cannot be directly deduced and compared with the averaged gradient given by Compton *et al.*.

In a recent paper [4], we proved that the model developed previously could be applied to electrolytic media containing both species A and B flowing in the laminar or turbulent regime. As predicted by [1, 2], experiments showed that the duration of transient phenomena was much longer when the electrode is large and when the wall velocity gradient is low. Nevertheless, the observed discrepancy between theoretical prediction and practice led us to investigate other numerical methods for solving the mass balance equation. Among the various numerical tools available for the solution of partial differential equations, calculation packages developed in the domains of heat transfer and chemical reaction engineering are not often used for electrode processes because of the complex boundary conditions at the electrodes. Nevertheless, the present case involves very simple initial and electrode conditions, with regard to the assumptions made. Therefore two different computer packages have been tested and have allowed the time variation of concentration of A as a function of the spatial coordinate and also the variation of reduced current density to be determined. Both software packages yielded comparable results which are in good agreement with experimental data described in a companion paper.

2. Theory

This section is dedicated to a brief description of the model presented previously [1, 2, 4] and to the techniques used for solving the partial differential equation relevant to the mass balance.

2.1. *Model*

Consider a simple Nernstian reversible electrode reaction A + e $\rightarrow$ B. The model relies upon weakly restrictive assumptions: migration effects have been neglected owing to a large excess of supporting electrolyte; the flow is postulated to be fully established and the cell dimensions render negligible the contribution of axial diffusion. Lastly, the diffusion coefficients of both species A and B have identical values. Therefore, the convective diffusion equation describing the variation of concentation for compound j is written in the form:

$$\frac{\partial C_j}{\partial t} = D\frac{\partial^2 C_j}{\partial y^2} - u\frac{\partial C_j}{\partial x} \tag{1}$$

Consider the linear velocity profile $u = sy$, where the wall velocity gradient is assumed to be constant. Dimensionless variables are defined as follows:

$X = x/L$; $Y = y(sL^{-1}D^{-1})^{1/3}$ and $\theta = t(Ds^2L^{-2})^{1/3}$

and

$$\mathbf{C}_j = C_j/C_{jb} \tag{2}$$

where L denotes the electrode length and s is the wall velocity gradient. Equation 2 is therefore expressed in the reduced form:

$$\frac{\partial \mathbf{C}_j}{\partial \theta} = \frac{\partial^2 \mathbf{C}_j}{\partial Y^2} - Y\frac{\partial \mathbf{C}_j}{\partial X} \tag{3}$$

with the boundary conditions:

$$\theta = 0 \quad Y \geqslant 0 \qquad \mathbf{C}_j = 1 \tag{4a}$$

$$\theta > 0 \quad Y \longrightarrow \infty \qquad \mathbf{C}_j \longrightarrow 1 \tag{4b}$$

$$\theta > 0 \quad Y = 0 \qquad \mathbf{C}_j = \mathbf{C}_{je} \tag{4c}$$

$$\theta > 0 \quad X < 0 \text{ and } X > 1 \qquad \mathbf{C}_j = 1 \tag{4d}$$

The values for both electrode concentrations can be reached from the value of electrode overpotential and the Nernst law, taking into account the relationship between electrode and bulk concentrations [4]:

$$C_{Ae} + C_{Be} = C_{Ab} + C_{Bb} \tag{5}$$

However, the time variation of the cell current can be obtained from the only concentration gradient of the substrate and the problem can therefore be restricted to compound A. For the sake of simplicity, **C** will denote the concentration of A in the following text.

2.2. *Software*

Equation 3 has been solved through numerical techniques with the help of two different packages:

(i) Differential Systems Simulator, Version 2 (DSS/2) [5] relies upon the numerical method of lines. The fourteen integration algorithms implemented can be classified as Runge Kutta with explicit truncation error estimates. For the present study, several algorithms have been tested: Runge Kutta Euler which is first-order exact; Runge Kutta Tanaka-5 and Runge Kutta England which are both fifth-order exact. Owing to the explicit equations involved, these methods are known to be hardly suitable for stiff problems [6] and other numerical techniques such as implicit methods or Gear's algorithms are therefore preferred.

(ii) Odepack consists of several moduli corresponding to various types of systems of ordinary differential equations. This package, proposed by Hindmarch *et al.* [7, 8], is based on a modified Gear's method. In particular, LSODA modulus [8] is a vari-

ant version of the LSODE package (Livermore Solver for Ordinary Differential Equations) and automatically selects the right method for stiff or nonstiff systems.

2.3. *Integration techniques*

Equation 3 subject to boundary conditions 4 could not be directly solved because of numerical problems and the principles of the packages described above.

2.3.1. Boundary conditions. The integration is based on a finite difference technique in a finite $(X-Y)$ domain. Equation 4b could not, therefore, be taken into account and a limit for the reduced transverse coordinate denoted Y_{max} should be defined. The mass balance equation has to be solved in the vicinity of the electrode and the integration domain must comprise the diffusional boundary layer. As a consequence Y_{max} must be an overestimate for the dimensionless diffusional layer and calculations reported in Appendix 1 show that a Y_{max} value of 3 represents a satisfactory integration limit.

On the other hand, boundary condition 4c allows a discontinuity to appear for electrode concentrations at time $t = 0$. This discontinuity does not have physical meaning and can be a source of rapid divergence of the integration routine. Expression 4c was then modified by the simple exponential expression:

$$\theta > 0,\ Y = 0 \quad \mathbf{C} = \mathbf{C}_e + (1 - \mathbf{C}_e) \exp(-\theta/\tau) \tag{4e}$$

where τ is a time parameter to be adjusted. Values for τ down to 0.002 could be used, corresponding to fairly stiff variation of electrode concentrations upon closure of the electrical circuit.

2.3.2. Calculation mesh. The two-dimensional integration domain has been divided into 600 small elements: the electrode increment, ΔX, was 1/20 and the transverse coordinate increment, ΔY, was 1/10. Partial derivative functions were replaced by finite difference approximations in one direction of a two-dimensional array; approximations were calculated by five-point centred formulae which are fourth-order correct. Equation 3 was therefore transformed into a system of 600 ordinary differential equations.

2.4. *Concentration gradient and current density*

Solving the system leads to the time variation of the concentration profile $\mathbf{C}(X, Y)$ from which the reduced concentration gradient at the wall, $(\partial \mathbf{C}/\partial Y)_{Y=0}$ can be calculated (Appendix 2). Γ_w will denote this gradient in the following text.

Current density, i, is proportional to the wall concentration gradient $(\partial C/\partial y)_{y=0}$. The relationship between i and Γ_w depends on the value for s, solely affected by the hydrodynamics in the cell. The ratio of the gradients averaged over the electrode at time t and under steady-state conditions, $\overline{\Gamma}_w/\overline{\Gamma}_{w\infty}$, is identical to the ratio of the transient and steady-state cell currents, I/I_∞.

3. Results

3.1. *General aspects*

Results presented below are for the case of diffusional control, corresponding to a zero wall concentration of the electroactive species A.

Calculations could be carried out with minicomputers, Bull Mini 6-92 or Sun Workstation 3/50. Equation 3, taking into account boundary conditions 4a, 4d and 4e, was integrated for θ ranging 0–5; the CPU time required varied from 15 min or so in the case of LSODA package to approximately 2 hours with DSS/2 software. LSODA was employed without defining explicit formula for the jacobian matrix elements.

The influence of several 'operating' conditions on the obtained results have been tested: integration step, integration algorithm and, eventually, calculation mesh. With regard to mesh size, a satisfactory convergence could be obtained for a coarse mesh in the integration domain ($\Delta X = \Delta Y = 1/6$) if a fifth-order algorithm was used. Nevertheless, the thinner calculation mesh described above allowed more accurate values for concentration gradients. Besides, no integration divergence was observed for an integration step value below 10^{-3}, whatever the numerical algorithm considered. Both packages led to nearly identical concentration profiles and the maximal deviation observed was below 5%. With respect to DSS/2 software, fifth-order algorithms were preferred to the simple Euler procedure despite the larger calculation time required; both Tanaka-5 and England yielded the same concentration variations within the deviation range $\pm 0.5\%$.

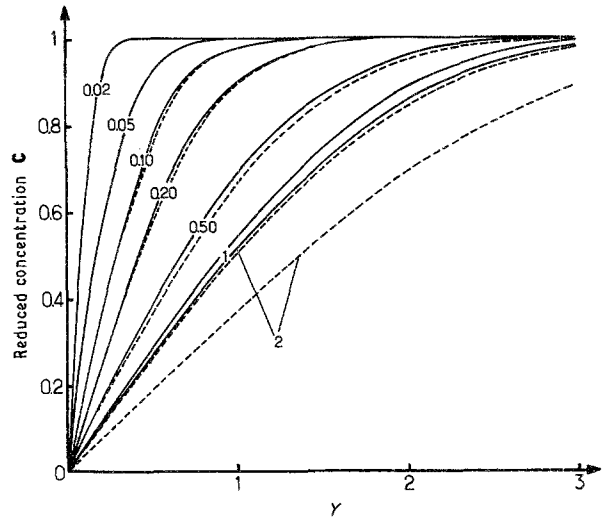

Fig. 1. Transient concentration profiles at the outlet of the reactor ($X = 1$) for various values of the reduced time θ; diffusional control assumed; (– – –) concentration profile after Cottrell's law.

Figure 1 displays an example of the concentration profile formation at the outlet of the channel electrode reactor ($X = 1$): the transient phenomenon is observed to occur mainly for reduced time values below unity and the reactor operates under steady-state conditions as θ exceeds 3. In addition, concentration profiles are developed for reduced coordinate values Y below 3 as $\mathbf{C}_{Y=3}$ is larger or equal to 0.96; this fact validates the estimation for the $(X-Y)$ domain limits and demonstrates that the integration is actually performed in the entire diffusional boundary layer. The presented profiles are compared with corresponding profiles predicted by Cottrell's well-known equation. Solving this differential mass balance equation, regardless of convective phenomena, led to the expression for the reduced concentration:

$$\mathbf{C} = \operatorname{erf}(Y/2\sqrt{\theta}) \tag{6}$$

Figure 1 shows that Expression 6, which is not x dependent, represents a good approximation for the actual substrate concentration calculated at the reactor outlet as θ is below 0.20; however, Equation 6 cannot be used for larger time values.

3.2. *Concentration gradients and cell current*

Two main parameters govern the concentration profiles and resulting current density: time and the considered position at the electrode. Both influences are discussed separately.

3.2.1. Variation with time. Compton *et al.* [1] established the expression for the steady state concentration gradient at the wall averaged over the electrode area, $\overline{\Gamma}_{w\infty}$:

$$\overline{\Gamma}_{w\infty} = \frac{c_0}{a_0\Gamma(5/3)} \tag{7}$$

where a_0 and c_0 are the first coefficients of the power series developments of the Airy function and of its logarithmic derivative, respectively. Values of these coefficients lead to

$$\overline{\Gamma} = 0.80\,660$$

The average concentration gradients, $\overline{\Gamma}_w$, were obtained through numerical integration of the axial profile of concentration gradients, Γ_w, and Fig. 2 reports their variation with reduced time. As observed for concentration profiles, steady-state conditions seem to hold for $\theta > 1$ as the average gradient differs by less than 2% from its steady-state limit. In perfect agreement with Compton's theory, this limit, calculated by both packages, was found to equal 0.812 and 0.816.

However, the rate of decrease of the absolute value of the concentration gradient largely depends on the calculation technique; numerical methods based on finite differences yield a decreasing rate twice as large as that predicted previously (Fig. 2). As an example, the reduced time, θ_2, taken for the current to fall from its initial value to twice the final steady-state value is close to 0.35 according to [1] and 0.13 according to the present work.

The variation of the average concentration gradient can be compared with both Cottrell's current vari-

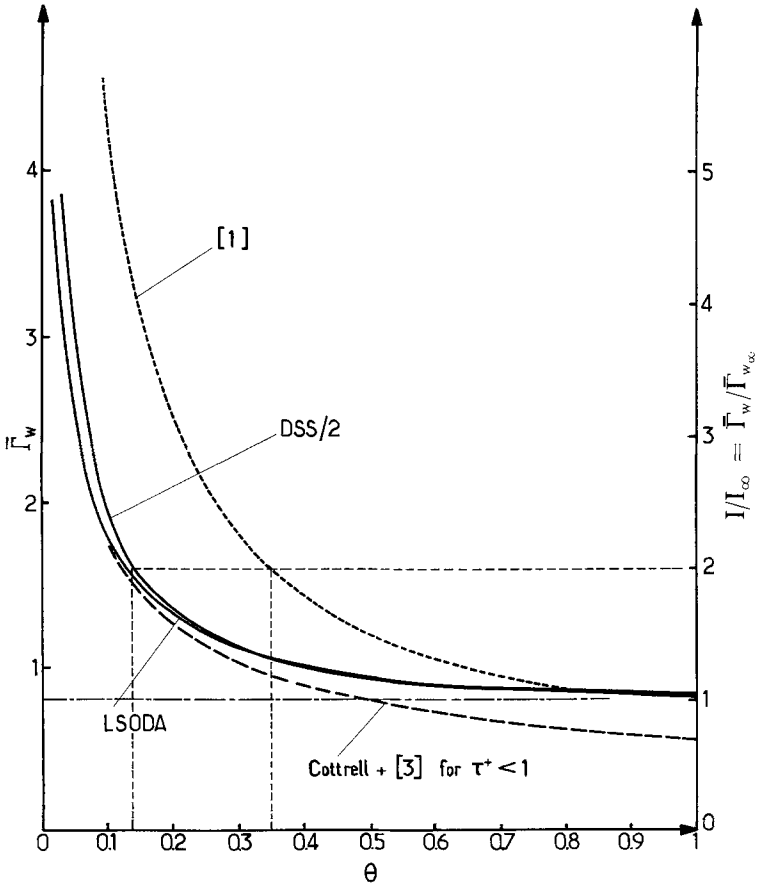

Fig. 2. Time variations of the reduced concentration gradient at the wall averaged over the electrode, $\overline{\Gamma}_w$, and the ratio $\overline{\Gamma}_w/\overline{\Gamma}_{w\infty}$ identical to the ratio I/I_∞; (9) and (11) in dotted line.

ation and the results of Soliman and Chambré: their approach shows that, for short times, the heat flux at the abscissae x is given by the expression:

$$\frac{(\partial T/\partial y)_{y=0}}{(\partial T/\partial y)_{y=0,\infty}} = 1.0480/\sqrt{\tau^+} \qquad (8)$$

where τ^+ is equal to $\theta/X^{2/3}$. Calculations presented in Appendix 3 demonstrate that Relation 8 yields the variation law for the reduced gradient of temperature, or concentration as follows:

$$(\partial \mathbf{T}/\partial Y)_{Y=0} \approx -0.5642/\sqrt{\theta} \qquad (9)$$

On the other hand, the wall concentration gradient calculated from Cottrell's equation is expressed as:

$$(\partial C/\partial y)_{y=0} = \frac{C_b - C_e}{(\pi Dt)^{1/2}} \qquad (10)$$

Under the assumption of diffusional control Equation 10 can be reduced to dimensionless form with the help of Relations 2

$$(\partial \mathbf{C}/\partial Y)_{Y=0} = \Gamma_w = 1/(\pi\theta)^{1/2} \qquad (11)$$

It can be observed that this gradient calculated without regard to hydrodynamics is relevant to the whole electrode surface and is proportional to the cell current in the case of motionless electrolyte. In addition, Expressions 9 and 11 are perfectly equivalent, as expected. These expressions, plotted as the dotted line in Fig. 2, are shown to be a good approximation for the solution of Equation 3 for reduced time θ below 0.2. During the first instants of diffusion layer formation, the concentration profile is very steep and the resulting second-order derivative concentration prevails over the convective term. As the layer is developed at the metal surface, the convective phenomena increase and equal the diffusional contribution and the concentration gradient tends to steady-state equilibrium, as a result.

3.2.2. Variation with electrode abscissae. Figure 3 reports the variation of the ratio of local and average gradient, $\Gamma_w/\bar{\Gamma}_w$, with the axial coordinate: the extent of dependence is observed to be an increasing function of time. For the first moments of the transient operation, the concentration profile is weakly affected by X and the axial distribution of gradient is fairly flat: the corresponding current density is almost uniform, except at the entrance to the reactor. As the concentration profile is nearly developed, the ratio tends to the asymptotic function $(\frac{2}{3}X^{-1/3})$ plotted as the dotted line in Fig. 3; it can be observed that the integral of the asymptotic function, calculated between 0 and 1, is obviously unity. The exponent of the limiting function can be explained as follows for the case of laminar flow: for such a flow, the wall velocity gradient does not depend on coordinates x or y and current density is therefore proportional to the wall gradient, Γ_w. Besides, in steady-state conditions, the diffusion layer thickness, δ, varies with $X^{1/3}$, corresponding to an axial decrease of current density with $X^{-1/3}$ under diffusion control.

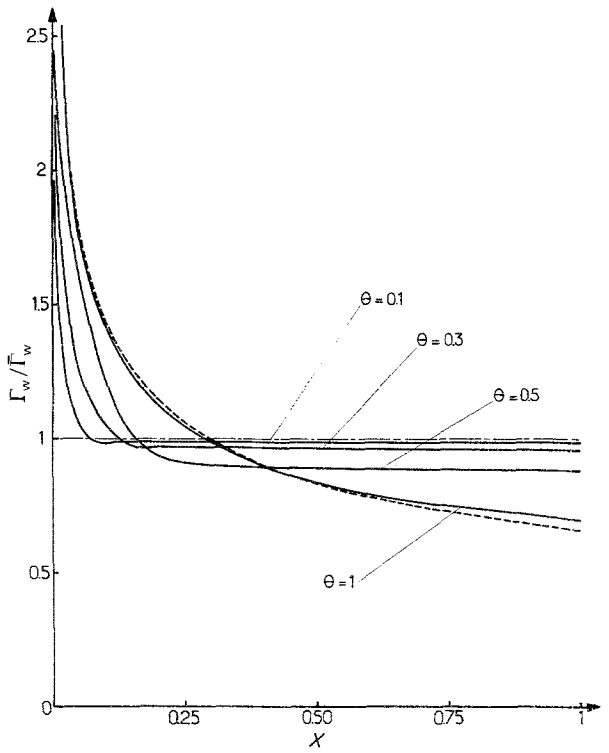

Fig. 3. Variation of the reduced wall concentration gradient $\Gamma_w/\bar{\Gamma}_w$ with the electrode abscissae for various values of θ.

For turbulent flow, the gradient variation with axial coordinate seem to be contradictory with mass transfer theory after which the mass transfer coefficient is not affected by electrode length. Equation 3, describing the mass balance near the electrode, has been established under the assumption that turbulence effects could be neglected in the diffusion layer [4]: the results obtained demonstrate that turbulent components of velocity and diffusion coefficients should be taken into account for a more rigorous treatment of fully turbulent flow.

4. Comparison with experimental results

The model predictions were compared with experimental results presented previously [4]. Experiments were carried out in a vertical channel electrode reactor divided into two symmetrical compartments whose dimensions were 5 × 40 × 85 mm. The current variations were observed for the reduction of potassium ferricyanide (5×10^{-3} M) in 1 M NaOH medium. Two carefully polished electrodes (dimensions 40 × 65 mm) were used; the fluid velocity was varied between 0.02 and 0.04 m s^{-1} and the corresponding Reynolds number was in the range 200–4000. Owing to the reactor dimensions, the wall velocity gradient could not be measured but was estimated from the mass transfer rate at the electrode or approximated to $(6u_m/b)$ in the case of laminar flow.

The model was applied to the transient of the channel reactor under laminar conditions (Fig. 4). Experimental and theoretical variations exhibit similar steady-state currents and current decays with time

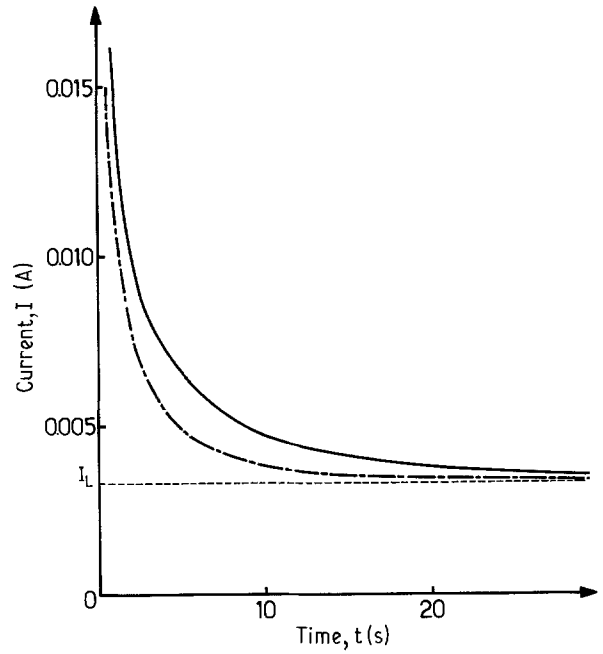

Fig. 4. Time variation of the cell current under diffusional control for $u_m = 0.0194\,m\,s^{-1}$; (——) experiment, (- - -) theoretical with $s = 6u_m/b$ (laminar flow).

despite a noticeable deviation; this discrepancy might be due to error in the s values estimated.

Although the simulation does not take into account possible turbulence phenomena near the electrode, comparison has been made in terms of overall current for the largest velocity values. The overall mass transfer coefficient, k_d, measured through the reduction of ferricyanide ion yielded estimates for the average wall velocity gradient with the help of mass and momentum transfer analogies. The analogies proposed by Lin *et al.* [9] or by Sandall *et al.* [10] are known to correlate both forms of transfer in a satisfactory manner for various hydrodynamic conditions in fully turbulent liquid flow and were, thereafter, selected. Consider the example of fluid velocity u_m equal to $0.284\,m\,s^{-1}$; the mass transfer coefficient was determined to be $1.51 \times 10^{-5}\,m\,s^{-1}$ and corresponding s values were estimated to be 385 and $710\,s^{-1}$ from Sandall's and Lin's models, respectively. As reduced time varies with $s^{2/3}$, the s range between both correlations (30% or so) corresponds to a time deviation close to 20% for a fixed current value. The variations of the cell current calculated on the basis of the two s values are observed to represent a good prediction for the transient of the reactor as the experimental decay lies between the theoretical curves (Fig. 5).

5. Conclusion

This paper describes prediction of the transient current induced by a potential step at a channel electrode. The validity of the results obtained with integration packages has been verified for short times by comparison with Cottrell's law and previous work dealing with heat transfer. In addition, predictive results can be successfully applied to an actual reactor as good agreement has been observed with experimental data. Although the simulation shows a dependance of the current density on the axial coordinate corresponding to a laminar flow near the electrode, the overal transient cell current can be predicted for more turbulent flow, provided the value of the velocity gradient is known.

Appendix 1

Equation 3 has to be solved in a finite domain which must comprise the diffusional boundary layer. Thus the following relationship has to be satisfied:

$$y_{max} > \delta \qquad \text{(A1)}$$

The thickness of the diffusional layer, δ, obviously depends on the hydrodynamics. In addition, the relationship between y and Y is a function of the wall velocity gradient and, therefore, of hydrodynamics.

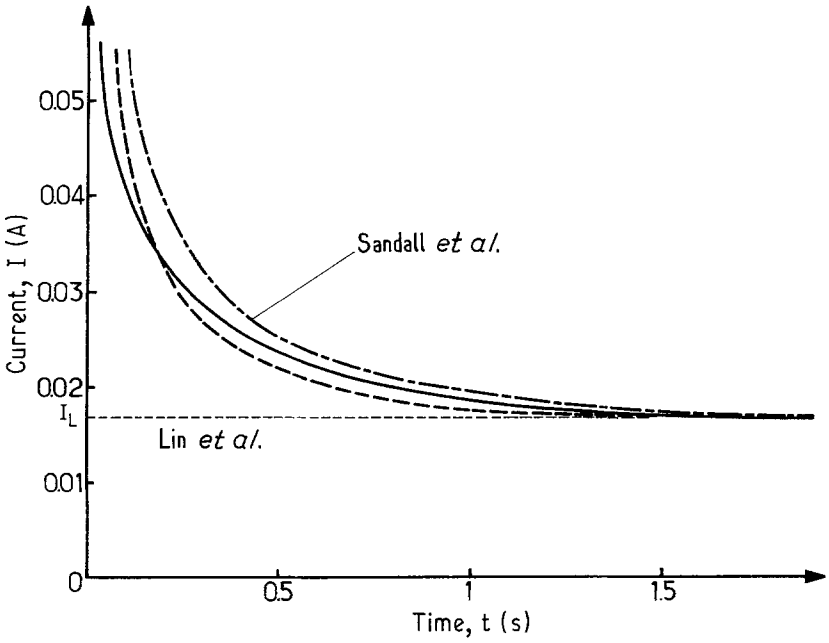

Fig. 5. Time variation of the cell current under diffusional control for $u_m = 0.284\,m\,s^{-1}$; (——) experiment, (- - -) theoretical with s estimates from Lin's or Sandall's analogies.

Estimates for Y_{max} have been calculated for both laminar and turbulent flow.

For the example of established laminar flow, mass transfer performance can be expressed as follows:

$$\mathrm{Sh} = k_d d_h/D = 1.85(\mathrm{Re\ Sc}\ d_h/x)^{1/3} \quad \text{(A2)}$$

where d_h is the hydraulic dimension of the cell and can be approximated by $(2b)$ if the cell width, w, is much larger that the cell depth, b. δ is an increasing function of abscissae and $\delta_L = \delta_{(x=L)}$ is given by

$$\delta_L = \frac{d_h}{1.85(\mathrm{Re\ Sc}\ d_h/L)^{1/3}} \quad \text{(A3)}$$

Taking into acount the expression for Reynolds and Schmidt numbers, the Condition A1 can be written in the form:

$$y_{max} > \frac{1}{1.85}\left(\frac{d_h DL}{u_m}\right)^{1/3} \quad \text{(A4)}$$

where u_m denotes the average fluid velocity. In the present case of laminar flow, the wall velocity gradient is $(6u_m/b)$ and it can be deduced that the minimal value for the Y limit is close to 1.24.

For a fully turbulent flow, estimation of the minimum value for Y_{max} can be achieved through a mass–momentum analogy allowing correlation between δ and s. Calculations can be made on the basis of Sandall's analogy [10] which is representative of various turbulent flows. In the case of liquid flowing in a reactor, the analogy can be expressed in the approximate form:

$$\mathrm{St_M}/\sqrt{f/2} = k_d/u_m\sqrt{f/2)} = 0.08\,\mathrm{Sc}^{-2/3} \quad \text{(A5)}$$

with a truncation error below 15%. Moreover, s related to the friction factor $(f/2)$:

$$s = \frac{f}{2} - \frac{u_m^2}{v} \quad \text{(A6)}$$

Let Δ be the dimensionless thickness of the diffusion layer. Equations A5 and A6 yield the expression for Δ as a function of the Reynolds number, friction factor and cell dimensions:

$$\Delta = \frac{12.5}{\mathrm{Re}^{1/3}(f/2)^{1/6}}(d_h/L)^{1/3} \quad \text{(A7)}$$

The friction factor at the wall of a rectangular channel is a function of the Reynolds number according to the Blasius relation:

$$f/2 = 0.0395\,\mathrm{Re}^{-0.25} \quad \text{(A8)}$$

and leads to Equation A9

$$\Delta = 21.4\,\mathrm{Re}^{-0.292}(d_h/L)^{1/3} \quad \text{(A9)}$$

Neglecting the weak influence of the reactor dimensions in Equation A9 and considering Re values larger than 3000 for fully turbulent flow allows estimation of the minimum value for Y_{max}: $Y_{max} > 2.07$.

The approximate calculations presented for both laminar and turbulent flow show that the integration domain should comprise the diffusional layer for a Y_{max} value of 3.

Appendix 2

The wall concentration gradient $(\partial \mathbf{C}/\partial Y)_{Y=0}$, denoted Γ_w, is not directly available and can be estimated from the gradient value at $Y = \Delta Y$, $(\partial \mathbf{C}/\partial Y)_2$, and a second-order Taylor approximation:

$$\left(\frac{\partial \mathbf{C}}{\partial Y}\right)_1 = \Gamma_w = \left(\frac{\partial \mathbf{C}}{\partial Y}\right)_2 + \Delta Y\left(\frac{\partial^2 \mathbf{C}}{\partial Y^2}\right)_2 + \tfrac{1}{2}\Delta Y^2\left(\frac{\partial^3 \mathbf{C}}{\partial Y^3}\right)_2 + \ldots \quad \text{(A10)}$$

The values of the first and the second derivative functions are provided by the packages; the third order term can be reached through a three-point finite difference approximation and second-order correction:

$$\left(\frac{\partial^3 \mathbf{C}}{\partial Y^3}\right)_2 = \frac{1}{2\Delta Y}\left[-3\left(\frac{\partial^2 \mathbf{C}}{\partial Y^2}\right)_2 + 4\left(\frac{\partial^2 \mathbf{C}}{\partial Y^2}\right)_3 - \left(\frac{\partial^2 \mathbf{C}}{\partial Y^2}\right)_4\right] \quad \text{(A11)}$$

Appendix 3

For short times, Soliman and Chambré established the approximate expression for the variation of the heat flux at x as:

$$\frac{(\partial T/\partial y)_{y=0}}{(\partial T/\partial y)_{y=0,\infty}} = 1.0480/\sqrt{\tau^+} \quad \text{(A12)}$$

where $\tau^+ = \theta/X^{2/3}$. In addition, the steady-state wall heat flux was calculated by Tribus and Klein [11] as:

$$(\partial T/\partial y)_{y=0,\infty} = \frac{3^{1/3}(T_b - T_w)u_m \mathrm{Pr}^{1/3}}{\Gamma(1/3)x^{+1/3}v} \quad \text{(A13)}$$

where x^+ is a reduced abscissae defined as (xu_m^3/sv^2) after [3]; T_w and T_b are the temperatures at the wall and in the bulk solution respectively. Introducing the reduced temperature, T, equal to $(T - T_b)/(T_w - T_b)$, leads to the expression for the reduced temperature gradient at steady-state after rearrangement:

$$(\partial \mathbf{T}/\partial Y)_{Y=0,\infty} = \frac{-3^{1/3}}{\Gamma(1/3)X^{1/3}} \quad \text{(A14)}$$

taking into account the analogy between heat and mass transfer. Equations A12 and A14 make possible the expression for the time reduced gradient with the help of Equation 2

$$(\partial \mathbf{T}/\partial Y)_{Y=0} = \frac{-1.0480 \times 3^{1/3}}{\Gamma(1/3)\sqrt{\theta}} \quad \text{(A15)}$$

which can be approximated as $(\partial \mathbf{T}/\partial Y)_{Y=0} = 0.5642/\sqrt{\theta}$

References

[1] R. G. Compton and P. J. Daly, *J. Electroanal. Chem.* **178** (1984) 45.

[2] R. G. Compton and P. R. Unwin, *J. Electroanal. Chem.* **205** (1986) 1.

[3] M. Soliman and P. L. Chambré, *Int. J. Heat. Mass Transfer* **10** (1967) 169.

[4] F. Lapicque, J. M. Hornut, A. Louchkoff and A. Storck, *J. Appl. Electrochem.* **19** (1989) 195.
[5] W. E. Schiesser, 'Differential Systems Simulator Version 2, an Introduction to the Numerical Method of Lines. Integration of Partial Differential Equations'. Lehigh University, Betleem, U.S.A.
[6] B. A. Finlayson, 'Non-linear Analysis in Chemical Engineering', MacGraw Hill, New-York (1980).
[7] A. C. Hindmarsh, UCID-30059-Rev 1 Computer Documentation, Lawrence Livermore Laboratory, University of California, USA (1975); ACM Signum Newsletter, Vol. 15 (1980) p. 10.
[8] L. R. Petzold, 'Automatic Selection of Methods for Solving Stiff and Nonstiff systems of ODE', Sandia National Laboratory Report SAND 80–8230, Sept. (1980).
[9] C. S. Lin, E. B. Benton, H. L. Gaskill and G. L. Putnam, *Ind. Eng. Chem.* **43** (1951) 2136.
[10] O. C. Sandall, O. T. Hanna and P. R. Mazet, *Can. J. Chem. Eng.* **58** (1980) 443.
[11] M. Tribus and J. Klein, 'Forced convection from nonisothermal surfaces', Heat Transfer Symposium, University of Michigan (1952) p. 221.